PROCEEDINGS OF SCIENCE

Latest results from the HERMES experiment

Charlotte Van Hulse*, on behalf of the HERMES Collaboration
University of the Basque Country – UPV/EHU , Spain
E-mail: cvhulse@mail.desy.de

HERMES collected a wealth of deep-inelastic scattering data using the 27.6 GeV polarized HERA lepton beam and various pure, polarized and unpolarized, gaseous targets. This unique data set opens the door to various measurements sensitive to the multi-dimensional structure of the nucleon. Among them are semi-inclusive deep-inelastic scattering measurements of azimuthal modulations sensitive to the Sivers, Boer-Mulders, and Worm-gear distributions as well as of light-meson multiplicities, all providing information on the three-momentum-dependent quark distributions. Knowledge on the quark distribution as a function of longitudinal momentum and transverse position in impact-parameter space can be accessed through deeply virtual Compton scattering, in particular through its improved, background-free measurement via recoil-proton detection. The various measurements of the observables providing insight into the multi-dimensional nucleon structure are presented.

The European Physical Society Conference on High Energy Physics -EPS-HEP2013
18-24 July 2013
Stockholm, Sweden

*Speaker.

PoS(EPS-HEP 2013)465

1. Introduction

The HERMES experiment at DESY in Hamburg (Germany) collected data from 1995 until 2007 using the 27.6 GeV HERA lepton beam. In the experiment, longitudinally polarized electrons or positrons were scattered off stationary gaseous hydrogen, deuterium, helium, or heavier targets, with hydrogen longitudinally or transversely polarized or unpolarized, deuterium and helium longitudinally polarized or unpolarized, and the heavier targets unpolarized. The scattered lepton and particles produced in the collision were detected by a forward spectrometer. Here, lepton-hadron separation was performed by a transition-radiation detector, a preshower, and a calorimeter, with an identification efficiency exceeding 98% and a misidentification contamination below 1%. Hadron identification was performed by a ring-imaging Cherenkov detector, allowing the discrimination of pions, kaons, and protons. In the last two years of data collection, a recoil detector was installed around the target cell, filled with unpolarized hydrogen or deuterium, in order to detect low-momentum particles, outside the acceptance of the forward spectrometer. This detector consisted of a silicon-strip detector, a scintillating-fibre tracker, and a photon detector.

Data collected on unpolarized targets were used to extract multiplicities in semi-inclusive deep-inelastic scattering (DIS). These multiplicities provide information on the fragmentation of quarks into final-state hadrons. The measurement of pion and kaon multiplicities from data taken with a hydrogen and deuterium target is presented in section 2. The extracted kaon multiplicities were also used to re-evaluate the strange-quark distribution. This is discussed in the same section.

Extending the analysis to the non-collinear distribution of hadrons, i.e., also taking into consideration their azimuthal distribution, provides access to the Boer-Mulders distribution and the Collins fragmentation function. The former describes the distribution of transversely polarized quarks in an unpolarized nucleon, and correlates the transverse momentum of the quarks with their spin, while the latter describes the fragmentation of a transversely polarized quark into an unpolarized hadron. Results sensitive to these two quantities are presented in section 3.

Semi-inclusive DIS off a transversely polarized target allows, among others, to access the Sivers and Worm-gear distributions. The Sivers distribution describes the distribution of unpolarized quarks in a transversely polarized nucleon, correlating quark transverse momentum and quark transverse spin, while the Worm-gear distribution describes the distribution of longitudinally polarized quarks in a transversely polarized nucleon, taking into consideration quark transverse momentum. Measurements accessing these distributions are discussed in section 4.

Turning to exclusive reactions, deeply virtual Compton scattering (DVCS) provides the cleanest access to generalized parton distributions (GPDs). The Fourier transforms in impact-parameter space of these probability amplitudes describe the distribution of quarks as a function of their longitudinal momentum and transverse position. At HERMES various azimuthal asymmetries have been extracted with data collected using a (longitudinally polarized) positron and electron beam on hydrogen and deuterium targets in various polarization states (see, e.g., Refs. [1–6]), allowing access to different GPDs. Without the usage of the recoil detector, the selected data sample contains a 12% contribution from associated production, where, e.g., the proton is excited to a Δ resonance. With the active detection of protons (and pions) using the recoil detector, this contribution of associated production is reduced to a negligible level. In addition the recoil detector allows the measurement of associated DVCS. Results on the latter two measurements are discussed in section 5.

PoS(EPS-HEP 2013)465

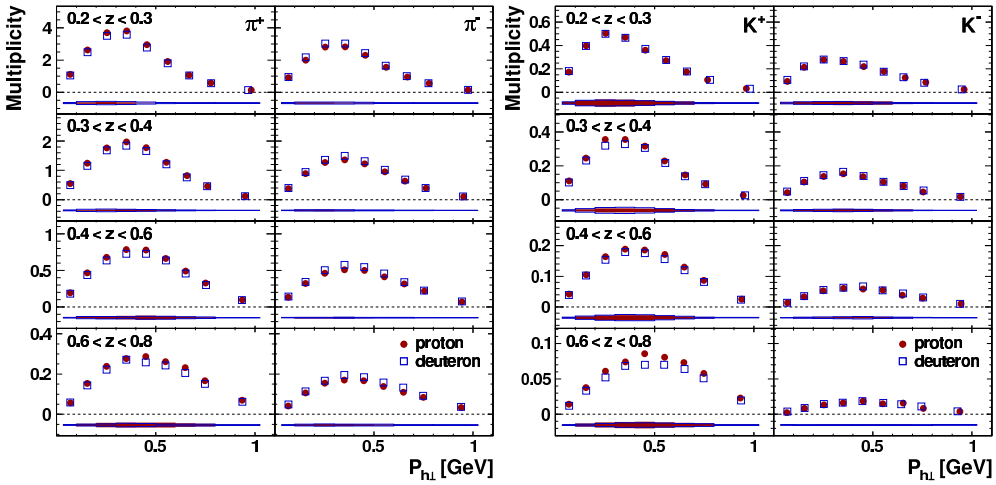

Figure 1: Charge-separated pion (left panel) and kaon (right panel) multiplicities as a function of $P_{h\perp}$ and z for protons (filled circles) and deuterons (open squares). Statistical uncertainties are represented by the error bars; systematic uncertainties are represented by the error bands.

2. Charge-separated pion and kaon multiplicities and re-evaluation of the strange-quark distribution

Hadron multiplicities, i.e., hadron numbers per DIS event, were measured in three-dimensional bins in $(Q^2, z, P_{h\perp})$ and in $(x_B, z, P_{h\perp})$ for charge-separated pions and kaons, using an unpolarized hydrogen and deuterium target [7]. Here $-Q^2$ represents the squared four-momentum of the virtual photon that mediates the lepton-nucleon interaction, z denotes, in the target-rest frame, the fractional hadron energy with respect to the virtual-photon energy, $P_{h\perp}$ the magnitude of the hadron momentum-component transverse to the virtual-photon three-momentum in the plane spanned by the three-momenta of the virtual photon and hadron (hadron-production plane), and x_B the x-Bjorken variable. The experimentally extracted multiplicities are corrected for QED radiative effects, limited geometric and kinematic acceptance of the spectrometer, losses due to decay in flight and secondary strong interactions, and finite detector resolution using an unfolding procedure, based on a LEPTO and JETSET Monte-Carlo simulation, similar to the procedure described in Ref. [8]. Obtained results are presented with and without the subtraction of the contribution originating from exclusive vector-meson production. The pion and kaon "Born" multiplicities, corrected for exclusive vector-meson production, are presented in figure 1 for protons (filled circles) and deuterons (open squares), as a function of $P_{h\perp}$ for various intervals in z.

As can be seen in figure 1, π^+ multiplicities for protons are larger than for deuterons, whereas for π^- the opposite is true. In addition, the ratio of the π^+ and π^- multiplicities on proton (deuteron) ranges from 1.2 (1.1), in the first z bin, to 2.6 (1.8), in the last z bin. These observations can be understood by the dominance of scattering off a u-quark and a subsequent favored fragmentation of a u-quark into a π^+ over an unfavored fragmentation of a u-quark into a π^-, together with the increased d-quark content in deuterons in conjunction with a favored d-quark to π^- fragmentation. For kaons an analogous behavior is observed in the comparison of the multiplicity ratio of both kaon types and in the comparison of K^+ multiplicities for protons and deuterons. However, the K^- multiplicities seem to be insensitive to the target type. These results reflect the

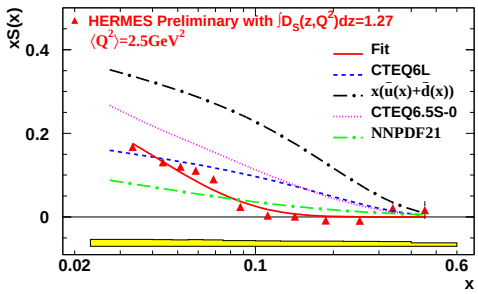

Figure 2: The strange-parton distribution $x_B S(x_B)$ (with x_B labeled as x) obtained from the measured HERMES multiplicities for charged kaons, evolved to $Q^2 = 2.5$ GeV^2, assuming the z-integrated kaon fragmentation function to be equal to 1.27 ± 0.13. The red solid curve is a result of a fit of the form $x_B^{-0.867} e^{-x_B/0.033}(1-x_B)$; the blue dashed curve gives $x_B S(x_B)$ from CTEQ6L; the black dashed-dotted curve gives the sum of the light antiquarks from CTEQ6L; the magenta dotted curve gives $x_B S(x_B)$ from CTEQ6.5S-0 [11]; the green dashed-dotted curve gives $x_B S(x_B)$ from the neural-network PDFs set NNPDF21 [12]. The band at the bottom represents the systematic uncertainties.

fact that K^-, being composed of valence quark types present in the nucleon only as sea quarks, can not be produced through favored fragmentation of nucleon valence quarks.

Similar considerations can also explain the observed transverse-momentum distributions from figure 1. The transverse hadron momentum reflects both the intrinsic transverse momentum of the struck quark inside the nucleon and the transverse momentum it acquires during the fragmentation process. As can be seen, negative kaons exhibit a broader multiplicity distribution than positive kaons and pions. This can reflect a more complicated hadronization process for negative kaons. Considering for example the LUND model, which models the fragmentation process in terms of string breaking, unfavored fragmentation is characterized by at least one more string break in comparison with favored fragmentation, resulting in a broader distribution of the transverse momentum.

Based on the above discussed multiplicities, a new extraction at leading-order in α_S of the strange-quark distribution $S(x_B) = s(x_B) + \bar{s}(x_B)$ was performed. A previous extraction of this distribution [9] was based on multiplicities for which the above described unfolding procedure was only carried out one dimensionally in x_B. The three-dimensional unfolding procedure resulted in significant changes for the obtained multiplicities. The newly extracted strange-quark distribution $x_B S(x_B)$ evolved to $Q^2 = 2.5$ GeV^2 is shown in figure 2. For this extraction, the non-strange-quark distribution from CTEQ6L was used, and the value for the z-integrated kaon fragmentation function $S(x_B) \to K = K^+ + K^-$ was chosen to be 1.27 [10]. The latter only enters as a normalization factor. Irrespective of its chosen value, the shape of the strange-quark distribution is in contradiction with the predictions.

3. Azimuthal distributions of charge-separated identified hadrons

When considering the non-collinear semi-inclusive DIS cross section, two additional structure functions appear in comparison with the collinear cross section. One appears at leading twist, with a $\cos(2\phi)$ modulation, and the other at sub-leading twist, with a $\cos(\phi)$ modulation. The angle ϕ denotes the angle between the lepton-scattering plane, i.e., the plane defined by the three-momenta of the incoming and scattered lepton, and the hadron-production plane, defined previously. The

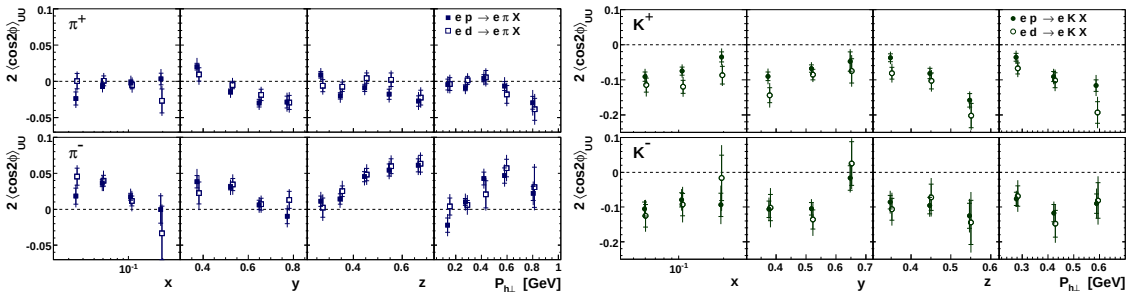

Figure 3: Charge-separated $\cos(2\phi)$ moments for pions (left panels) and kaons (right panels) versus x_B (here labeled as x), y, z, and $P_{h\perp}$ for protons (filled symbols) and deuterons (open symbols). Statistical uncertainties are represented by the inner error bars, while the total error bars represent the quadratic sum of statistical and systematic uncertainties.

$\cos(2\phi)$ term is a convolution of the Boer-Mulders distribution function and the Collins fragmentation function. The sub-leading twist structure function contains this same contribution together with a term related to the Cahn effect as well as quark-gluon-quark correlations.

The $\cos(\phi)$ and $\cos(2\phi)$ moments were extracted from data collected on a hydrogen and deuterium target, using a fully differential unfolding procedure in x_B, y, z, and $P_{h\perp}$ in order to eliminate moments induced by higher-order QED effects or detector acceptance [8]. Here y represents, in the target-rest frame, the fractional virtual-photon energy with respect to the beam-lepton energy.

In figure 3 the extracted $\cos(2\phi)$ moments projected in bins of x_B, y, z, and $P_{h\perp}$ are presented for π^+ (left top panel), π^- (left bottom panel), K^+ (right top panel), and K^- (right bottom panel) for data collected on proton (filled symbols) and deuterium (open symbols). As can be seen, the pion $\cos(2\phi)$ moments for data collected on hydrogen and on deuterium are compatible. This hints at similar Boer-Mulders distributions for u-quarks and d-quarks. On the other hand, positive moments for π^- and small but negative moments for π^+ are observed. This is compatible with a favored Collins fragmentation function (e.g., $u \to \pi^+$) with equal magnitude but opposite sign compared to the unfavored Collins fragmentation function (e.g., $u \to \pi^-$), as obtained from the measurements related to the transversity distribution. For kaons large, negative amplitudes are observed, with the K^- amplitude similar to the K^+ amplitude, both significantly larger than the pion amplitudes. These differences could, among others, be attributed to a different Collins fragmentation function for kaon production from u-quarks and to the role of sea quarks.

4. Single-spin asymmetries off transversely polarized protons

Single-spin asymmetries measured from a transversely polarized proton show characteristic angular modulations. Each of the corresponding azimuthal amplitudes is related to convolutions of different distribution and fragmentation functions. The amplitude of the $\sin(\phi - \phi_S)$ modulation, with ϕ_S the azimuthal angle of the transverse component of the target spin with respect to the lepton scattering plane and about the virtual-photon direction, is interpreted as the convolution of the Sivers distribution function and the spin-independent fragmentation function. The amplitude of the $\cos(\phi - \phi_S)$ modulation is proportional to the convolution of the Worm-gear function $g_{1T}^{\perp}$ and the spin-independent fragmentation function. These two azimuthal amplitudes were extracted

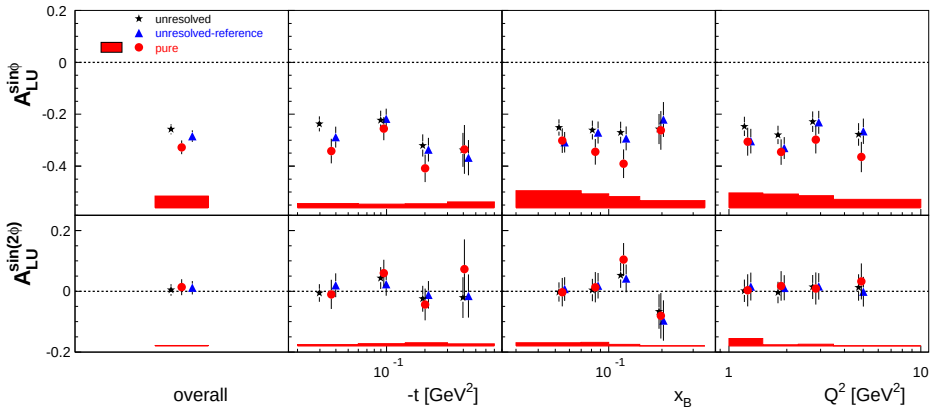

Figure 4: Amplitudes of single-charge beam-helicity asymmetry in DVCS shown in projections of $-t$, x_B, and Q^2. Statistical uncertainties are shown by error bars. The bands represent the systematic uncertainties of the amplitudes extracted from the pure sample. A separate scale uncertainty arising from the measurement of the beam polarization amounts to 1.96%. Shown are amplitudes extracted from a) the pure sample (red circles, shown at their kinematic values); b) the unresolved-reference sample (blue triangles, shifted to the right for better visibility); c) the unresolved sample (black stars, shifted to the left for better visibility).

from a transversely polarized hydrogen target as a function of x_B, z, and $P_{h\perp}$ for charged and neutral pions, and for charged kaons. The results on the Sivers amplitudes were published in Ref. [13], while for the Worm-gear amplitudes preliminary results are available.

The Sivers π^+ amplitude is significantly positive, rising with z and with $P_{h\perp}$ at low values of $P_{h\perp}$, after which it reaches a plateau at higher $P_{h\perp}$ values. Assuming u-quark dominance, this positive amplitude corresponds to a negative u-quark Sivers distribution function. The π^- amplitude is consistent with zero, which can be attributed to canceling contributions from the Sivers u- and d-quark distributions, while for the π^0 amplitude, isospin symmetry is fulfilled. In order to access the valence-quark Sivers distribution and in addition suppress contributions from exclusive vector-meson production, the (π^+–π^-)-Sivers amplitude was also extracted. The observed positive value of this pion-difference amplitude hints either at a valence d-quark distribution much larger than the valence u-quark distribution, or more probable, at a large negative valence u-quark Sivers distribution. The K^+ Sivers amplitude shows a similar kinematic dependence as the π^+ amplitude, but has a larger magnitude. This can hint at a non-trivial role of sea quarks. The K^- amplitude is also observed to be (slightly) positive.

The Worm-gear amplitudes for π^+ and K^+ show very small values, compatible with zero or slightly positive. For π^- positive values are observed, which as for the non-zero Boer-Mulders and Sivers amplitudes, signify a non-zero quark orbital angular momentum. For π^0 and K^- the amplitudes are compatible with zero.

5. Azimuthal asymmetries in elastic and associated deeply virtual Compton scattering

At the HERMES experiment, DVCS is accessed through azimuthal asymmetries, where the azimuthal angle ϕ is the angle between the photon-production plane and lepton-scattering plane.

These asymmetries probe the interference contribution of the DVCS and Bethe–Heitler processes. In the latter process, the real photon is not emitted by the quark probed by the virtual photon, but by the incident or scattered lepton. Before the installation of the recoil detector [14], the scattered lepton and real photon were detected by the forward spectrometer, while the recoiling proton was reconstructed through the determination of its missing mass. With active detection of the recoil proton by the recoil detector, the background contribution, which consists mainly of associated production (around 12%), could be reduced to a negligible level of below 0.2% [15].

In order to separate the effect of the recoil-detector acceptance from the removal of background, a so-called unresolved-reference sample was constructed. This sample consists of events where, based on the reconstructed photon and scattered-lepton kinematics using the forward spectrometer only, the recoiling proton was determined to lie within the recoil-detector acceptance. This unresolved-reference sample is estimated to contain 14% of associated background contribution. The asymmetries extracted from the data sample using the forward spectrometer only without considering the recoiling proton (unresolved), from the unresolved-reference sample, and from the data sample with active recoiling-proton detection (pure) are presented in figure 4, as a function of $-t$, x_B, and Q^2, with t the square of the difference between the initial and final four-momenta of the target proton. The leading twist-2 $\sin(\phi)$ asymmetry from the pure sample increases by 0.054 ± 0.016 with respect to the asymmetry from the unresolved-reference sample. This effectively indicates that the asymmetry from the associated process acts as a dilution. The same conclusion can be drawn from the measurement of associated DVCS, where events originating from associated production for the channels $ep \to e\gamma\pi^0 p$ and $ep \to e\gamma\pi^+ n$, around the Δ mass, are selected. Preliminary results for this asymmetry show a leading asymmetry amplitude compatible with zero. The sub-leading twist asymmetries for DVCS and associated DVCS are found to be compatible with zero.

References

[1] A. Airapetian et al. [HERMES Collaboration], JHEP **06** (2008) 066.

[2] A. Airapetian et al. [HERMES Collaboration], Nucl. Phys. B **829** (2010) 1.

[3] A. Airapetian et al. [HERMES Collaboration], JHEP **06** (2010) 019.

[4] A. Airapetian et al. [HERMES Collaboration], Phys. Lett. B **704** (2011) 15.

[5] A. Airapetian et al. [HERMES Collaboration], Nucl. Phys. B **842** (2011) 265.

[6] A. Airapetian et al. [HERMES Collaboration], JHEP **07** (2012) 32.

[7] A. Airapetian et al. [HERMES Collaboration], Phys. Rev. D **87** (2013) 074029.

[8] A. Airapetian et al. [HERMES Collaboration], Phys. Rev. D **87** (2013) 012010.

[9] A. Airapetian et al. [HERMES Collaboration], Phys. Lett. B **666** (2008) 446.

[10] D. de Florian, R. Sassot, and M. Stratmann, Phys. Rev. D **75** (2007) 114010.

[11] H. L. Lai et al., JHEP **04** (2007) 089.

[12] R. D. Ball et al. [NNPDF Collaboration], Nucl. Phys. B **855** (2012) 153.

[13] A. Airapetian et al. [HERMES Collaboration], Phys. Rev. Lett. **103** (2009) 152002.

[14] A. Airapetian et al., JINST **8** (2013) P05012.

[15] A. Airapetian et al. [HERMES Collaboration], JHEP **10** (2012) 042.

PoS(EPS-HEP 2013)465